Journal of Advanced Research (2014) 5, 219–242

Cairo University

Journal of Advanced Research

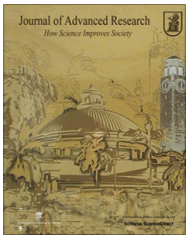

ORIGINAL ARTICLE

Proteomics of old world camelid (*Camelus dromedarius*): Better understanding the interplay between homeostasis and desert environment

Mohamad Warda [a,b,*], Abdelbary Prince [a], Hyoung Kyu Kim [c], Nagwa Khafaga [d], Tarek Scholkamy [e], Robert J. Linhardt [f], Han Jin [c]

[a] *Department of Biochemistry, Faculty of Veterinary Medicine, Cairo University, Giza, Egypt*
[b] *Biotechnology Center for Services and Researches, Cairo University, Giza, Egypt*
[c] *National Research Laboratory for Mitochondrial Signaling, Department of Physiology, Cardiovascular and Metabolic Disease Center, Inje University, Busan 614-735, Republic of Korea*
[d] *Animal Health Research Institute, Dokki, Giza, Egypt*
[e] *Field Investigation Department, Animal Reproduction Research Institute, Giza, Egypt*
[f] *Center for Biotechnology and Interdisciplinary Studies, Rensselaer Polytechnic Institute, Troy, NY 12180, USA*

ARTICLE INFO

Article history:
Received 22 January 2013
Received in revised form 4 March 2013

ABSTRACT

Life is the interplay between structural–functional integrity of biological systems and the influence of the external environment. To understand this interplay, it is useful to examine an animal model that competes with harsh environment. The dromedary camel is the best model that thrives under severe environment with considerable durability. The current proteomic study

Abbreviations: 2D, two-dimensional; MS, mass spectrometry; CHAPS, 3-(3-cholamidopropyl)-dimethylammoniopropane sulfonate; pI, isoelectric point; IPG, immobilized pH gradient; DTT, dithiothreitol; SDS, sodium dodecylsulfate; PAGE, polyacrylamide gel electrophoresis; TFA, trifluoracetic acid; MALDI, matrix assisted laser desorption ionization; CHCA, α-cyano-4-signal-to-noise; ACTH, adrenocorticotropic hormone; PMF, peptide mass finger printing; PDB, protein database; TOF, time of flight; hsp, heat shock protein; MAPK, map kinase; Dvl, dishevelled: scaffold protein involved in the regulation of the Wnt signaling pathway; DAPLE, Dvl-associating protein with a high frequency of leucine residues.

* Corresponding author. Tel.: +20 2 35682195/35720399; fax: +20 2 35725240/35710305.
E-mail address: maawarda@eun.eg (M. Warda).

Peer review under responsibility of Cairo University.

Production and hosting by Elsevier

http://dx.doi.org/10.1016/j.jare.2013.03.004

Accepted 13 March 2013
Available online 20 March 2013

Keywords:
Camel
Proteome
Metabolism
Crystallin
Actin
Vimentin

on dromedary organs explains a number of cellular mysteries providing functional correlates to arid living. Proteome profiling of camel organs suggests a marked increased expression of various cytoskeleton proteins that promote intracellular trafficking and communication. The comparative overexpression of α-actinin of dromedary heart when compared with rat heart suggests an adaptive peculiarity to sustain hemoconcentration–hemodilution episodes associated with alternative drought-rehydration periods. Moreover, increased expression of the small heat shock protein, α B-crystallin facilitates protein folding and cellular regenerative capacity in dromedary heart. The observed unbalanced expression of different energy related dependent mitochondrial enzymes suggests the possibility of mitochondrial uncoupling in the heart in this species. The evidence of increased expression of H + -ATPase subunit in camel brain guarantees a rapidly usable energy supply. Interestingly, the guanidinoacetate methyltransferase in camel liver has a renovation effect on high energy phosphate with possible concomitant intercession of ion homeostasis. Surprisingly, both hump fat tissue and kidney proteomes share the altered physical distribution of proteins that favor cellular acidosis. Furthermore, the study suggests a vibrant nature for adipose tissue of camel hump by the up-regulation of vimentin in adipocytes, augmenting lipoprotein translocation, blood glucose trapping, and challenging external physical extra-stress. The results obtained provide new evidence of homeostasis in the arid habitat suitable for this mammal.

Introduction

One humped camel (*Camelus dromedarius*) is a unique creature belonging to old world camelid that is adapted for desert life. These camels are found mainly in the Middle East with extension into tropical and subtropical areas. With drought becoming an increasingly common global threat, the peculiar nature of the camel to cope with hot and arid conditions makes it a strategically important animal. For 14 centuries, the dromedary has been referred to as a creature of wonder [1] having a special ability to both conserve and store water. The camel can survive long periods even after more than 40% loss of its body hydration. Moreover, camels can drink as much as 57 l of water in a short period of time; such rapid rehydration is capable of causing death to other mammals.

The camel shows a true rumination pattern of digestion, expected for a ruminating ungulates; however, based on anatomical and physiological issues, it is considered as pseudo-ruminant. The camel also has the highest blood glucose level among all ruminants with similarly high glucagon levels [2].

Dromedary red blood cells have an unusual elliptical shape, possibly to facilitate their flow in the dehydrated animal. These cells are also showing less osmotic fragility than red cells in other mammals [3]. Thus, the camel's red blood cells can withstand high osmotic variation without rupturing, even during rapid rehydration. This may result from altered membrane phospholipids distribution in its red blood cells [4]. Interestingly, as a result of having very efficient kidneys, the camel urine is as thick syrup and feces are so dry that they can fuel fires [5]

Sporadic research has led to discoveries of the uniqueness of dromedary, but our understanding of this domestic ruminant is still in its infancy. For example, camelids have an unusual immune system, where part of the antibody repertoire is devoid of light chains [6]. The role of the camel's immune system to their resistance to hot arid environments is currently unknown. The current systemic study attempts to elucidate the molecular basis for the adaptive changes required for the camel's survival in an arid environment. The peculiarity of dromedary camel among mammals turns our eyes to study

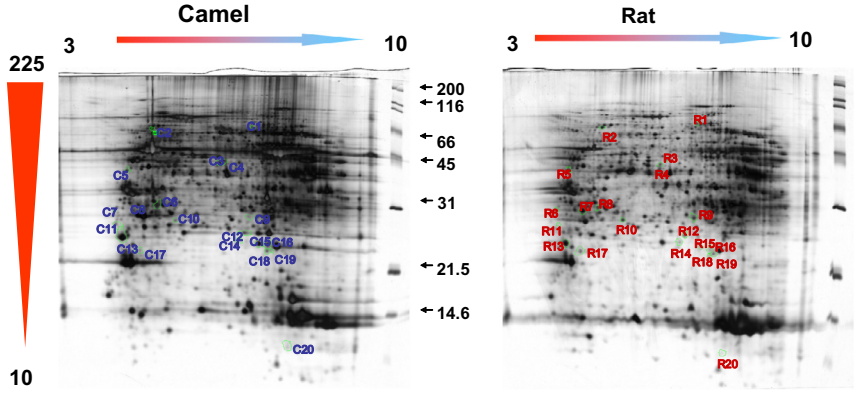

Fig. 1 Camel and rat heart proteins. In the 2D electrophoresis gel images (pH range: 3–10; with 10–225 MW range) approximately 1330 ± 95 spots were detected in each gel. The 20 significantly changed protein spots (marked spots) were selected for further MALDI-TOF MS analysis.

Table 1 Identified heart proteins in NCBI database search GI; NCBI gene bank ID, Mw; molecular weight, pi; isoelectric point, ΔC/R: relative change (camel/rat%).

Camel heart							
Spot no.	Identified AA sequence (MS/MS)	MATCHED protein	NCBI acc no.	Score	Mr/pI	Seq.cov	ΔC/R
C2	R.KPLVIIAEDVDGEALSTLVLNR.L R.AAVEEGIVLGGGCALLR.C	Heat shock protein 65 (*Mus musculus*)	51455	103	60903/5.48	7	49
C3	K.APIQWEER.N K.TPYTDVNIVTIR.E R.IAEFAFEYAR.N	NAD+ isocitrate dehydrogenase, alpha subunit (*Macaca fascicularis*)	1182011	183	36777/5.72	8	201
C4	MS, 11 PEPTIDE MATCHED FROM 65	3-Hydroxy-3-methylglutaryl Co-enzyme A reductase	2648815	64	47116/7.65		213
C5	K.IWHHTFYNELR.V K.SYELPDGQVITIGNER.F	Gamma non-muscle actin (*Oryctolagus cuniculus*)	1703	128	41729/5.30	7	35
C6	K.IWHHTMYNELR.V R.GYSFVTTAER.E K.SYELPDGQVITIGNER.F	Muscle actin (*Styela clava*)	10111	121	42040/5.29	9	280
C7	MS, 6 PEPTIDE MAT FROM TOTLA 65	Histone deacetylase HDAC3 (*Oryza sativa*)	50906299	49	56469/5.54		34
C8	K.AHGGYSVFAGVGER.T R.VALTGLTVAEYFR.D R.DQEGQDVLLFIDNIFR.F	ATP synthase beta subunit (*Oncorhynchus mykiss*)	76362315	215	18719/4.87	24	29
C11	R.VGWELLLTTIAR.T K.GITQEQMNEFR.A R.ASFNHFDR.R R.ETADTDTAEQVIASFR.I R.ILASDKPYILAEELR.R	Actinin, alpha 2 (*Homo sapiens*)	4501893	229	103788/5.31	6	984
C12, 13	K.IEFTPEQIEEFKEAFMLFDR.T K.ITYGQCGDVLR.A R.ALGQNPTQAEVLR.V K.NKDTGTYEDFVEGLR.V K.DTGTYEDFVEGLR.V	PREDICTED: similar to myosin light polypeptide 3	57101266	445	22355/5.02	29	286
C 15	R.RPFFPFHSPSR.L R.APSWIDTGLSEMR.L R.IPADVDPLAITSSLSSDGVL	Alpha B-crystallin chain	73954784	212	20054/6.76	28	773
C 16	R.RPFFPFHSPSR.L R.APSWIDTGLSEMR.L R.IPADVDPLAITSSLSSDGVL	Crystallin, alpha polypeptide 2-.Hsps	27805849	183	20024/6.76	28	321
C18	R.RPFFPFHSPSR.L R.APSWIDTGLSEMR.M	Alpha B-crystallin polypeptide 2 (*Rattus rattus*)	57580	99	19945/6.84	13	320

its proteome in comparison with rat. The choice of rat as a generally accepted central point mammalian model expands our scope of comparison beyond the limited frame of ungulates. Proteomic differences between different organs in the camel and the rat are examined by two-dimensional (2D) mass spectrometry (MS/MS)-enabled 2D electrophoresis. This study affords a better understanding of the interplay between mammalian homeostasis and a harsh environment.

Material and methods

Tissues

Healthy, clinically normal adult male one humped camels (*Camelus dromedarius*) were used in the study. Animals were kept on rest with food and water ad libitum one week before slaughtering. Liver, heart, brain, kidney, and hump fat from camels were collected and cut into thin slices at an authorized abattoir house (Giza District, Egypt). At least five animals were sampled for each organ. Samples were snap-frozen in liquid nitrogen and stored in −70°C until processing. The collection and use of these samples was approved by the Institutional Review Board of Egyptian Animal Health Affairs. Samples of the same organs were similarly prepared from rat (*Rattus norvegicus)* maintained at the animal care unit (Medical School – Inje University, Republic of Korea).

2D-gel electrophoresis and proteomics

Protein samples from camel organs were examined in parallel with rat control organs. Proteins were extracted for 2D gel electrophoresis using a 2D Quant kit (GE Healthcare) as

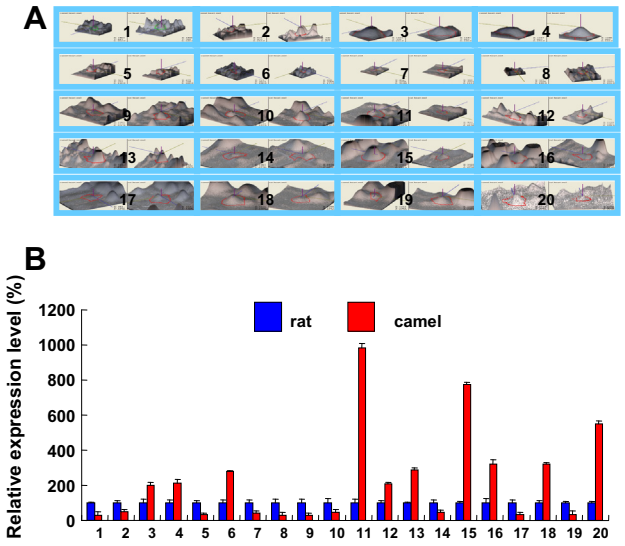

Fig. 2 Camel and rat heart proteins. (A) Enlarged three-dimensional electrophoresis spots images showing the 10 overexpressed and 10 under expressed protein spots. (B) Histograms quantify these protein spots. (The error bars represent the SEM of mean of at least three independent experiments, $p < 0.05$ vs control) (pH range: 3–10; with 10–225 MW range).

previously described [7] and described in Supplementary data sheet 1.

Image analysis

Silver-stained gels were scanned on a flatbed scanner (Umax PowerLook 1100; Fremont, CA, USA), and the resulting digitized images were analyzed using ImageMaster 2D Platinum software (GE Healthcare). At least three separate gels of the same organ from different animals were independently analyzed to increase experimental certainty. Further gel analysis was performed as previously described [8,9] and listed in Supplementary data sheet 2.

Protein mass analysis and identification

The selected stained spots were excised, destained, reduced and digested with trypsin. Peptides were analyzed with matrix assisted laser desorption ionization (MALDI) TOF/TOF mass spectrometer, 4700 Proteomics Analyzer (Applied Biosystems, Framingham, MA) for protein identification [7,8]. Resulting data were analyzed by GPS ExplorerTM 3.5 (Applied Biosystems) software. The proteins were identified by using MASCOT 2.0 search algorithm (Matrix Science, London) to search rodent subset of the National Center for Biotechnology Information (NCBI) protein databases.

Results

Data handling

The logical evaluation of the camel proteome is complicated by the absence of previously published genomic and proteomic data. Since rat (*Rattus norvegicus*) is a well known mammalian model with many Protein Data Bank (PDB) entries, the proteome of corresponding rat organs was used as the reference control. The protein levels in various camel organs were visualized on 2D electrophoresis gels. Based on an automated spot-counting algorithm (Image Master 2D Platinum), means of 1325 ± 95 protein spots were detected in the gel of the heart, liver, adipose tissue, kidney, and brain. All spots were distributed in the region of pI 4–9 and had relative molecular weights (MW) between 15 and 200 KDa. The protein spots in both camel and control gels were then excised from the gel and incubated with trypsin to digest the proteins in the gel, which were then analyzed by MALDI-time of flight (TOF) MS/MS.

Camel heart proteome

The camel heart proteome showed a well matched proteomic image to that of the rate heart control (Fig. 1 and Table 1). It is clear that actinin and alpha B-crystallin were markedly overexpressed in camel compared to that of the control (Fig. 2). In the 2D electrophoresis-MS/MS data, alpha B-crystallin in camel heart showed peptides (Fig. 3A) that covered both conserved domains of bovine alpha B-crystallin [*Bos taurus*] as well as the intervening peptides (57–69 amino acid residues). These results demonstrate a strong identity between camel and bovine alpha B-crystallin with possible two sites for phosphorylation. Despite a twofold increase in the expression of NAD+-dependent isocitrate dehydrogenase in camel heart when compared to the rat heart, there was a parallel down regulation of ATP synthase expression. Moreover, all the overexpressed proteins had acidic pIs.

Physical distribution of the camel proteome

Camel heart proteomic data closely matched its counterpart rat proteome. To amplify the differences in proteomic data from the remaining organs, each gel was divided into four quarters and proteins separated based on MW and pI. The relative abundance of proteins in each group was estimated from the total number spots, and the percent area in each quarter gel occupied by proteins as revealed by gel imaging. These data were then compared to the corresponding quarters in rat control for liver adipose tissue and kidney (Fig. 4A–C). Interesting, both adipose tissue and kidney proteomes shared a higher density of acidic proteins (pI < 7). While these acidic proteins are concentrated in the low molecular weight range in hump adipose tissue, in the kidney proteome, these acidic proteins displayed a wide range of molecular weights.

Camel liver proteome

The camel liver proteome was dissimilar to the rat liver control. An area of well defined dimensions (pH and MW) was selected in that showed marked similarity by visual and digital inspection (Fig. 5A). The protein spots within these clearly defined boundaries were then analyzed by MALDI-TOF MS or MS/MS. The proteins identified in camel proteome with no corresponding counterpart in the rat control are representative of overexpressed proteins. To determine the amino acid sequence of proteins of camel proteome that does not match with the known proteome MS database, the MS/MS was then performed.

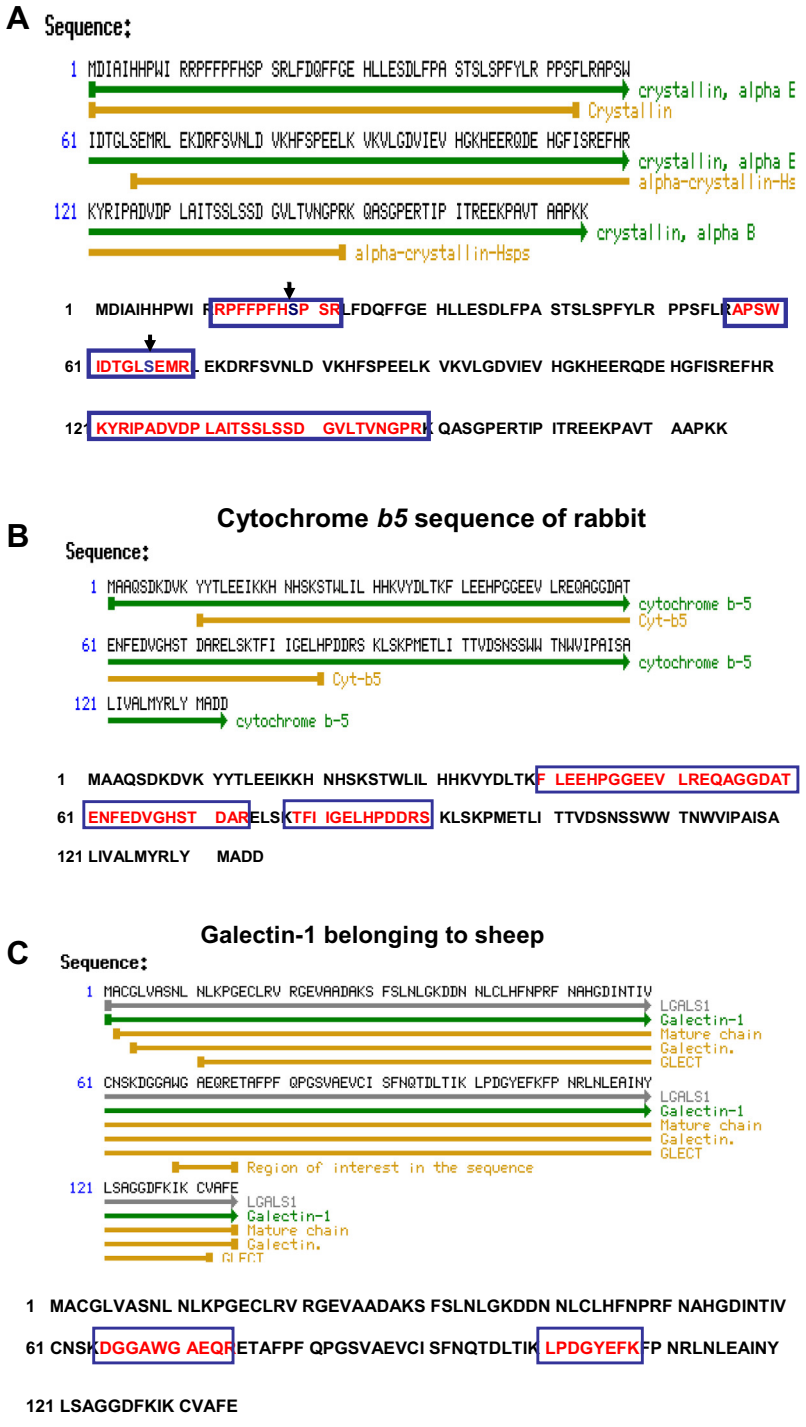

Fig. 3 Comparative analysis of sequence data obtained from the camel proteome. (A) α-B-crystallin belonged to bovine [Bos Taurus: gi:117384; top] showing the MS/MS-derived matched sequences in camel α-B-crystallin (red-marked with blue boxes sequences; bottom). The reported sequences in camel cover both conserved domains of bovine crystallin, α-B with marked identity to bovine one and possible two serine phosphorylation sites (indicated by arrows). (B) Cytochrome *b5* sequence of rabbit [*Oryctolagus cuniculus*] (top) and the shared amino acids sequence residues with that indicated by MS/MS data for camel adipose tissue (bottom). The shared sequences of camel with that of rabbit cytochrome b5 (gi:164785) are red-marked in blue boxes. The matched sequences carry different motives that responsible for the final enzyme activity. (C) Galectin-1 belonging to sheep [*Ovis aries*]. The sequence shown in red with blue framed box is the MS/MS-reported matched sequences in camel galectin-1. The specific region of interest in reported sequence of sheep (69–75 amino acid residues; WGAEQRE gi:3122339) is included with the matched camel sequence. (D) Bovine [*Bos Taurus*] phosphatidylethanolamine binding protein (gi:1352725) sequence. The MS/MS-matched amino acid residues in camel brain proteome (shown in red in blue framed box) are proved to have interspecies similarities in Beta-strand region (Res. # 62–70); hydrogen bonded turns (Res. # 71–72 and Res. # 94–95); helical region (97–99), and second Beta-strand region (Res. # 100–104).

Fig. 3 (*continued*)

The results of proteins were identified by MS, MS/MS for liver of camel and rat, respectively (Tables 2 and 3). The amino acid sequence from MS/MS of the guanidinoacetate methyltransferase (Fig. 6) matched this same protein in the corresponding NCBI peptide database. Among the determined set of liver proteins, a total 13 proteins were identified by MS to be over 70 (Mowse score) and/or over 34 in MS/MS peptide sequencing. The liver proteome showed differential expression of metabolic enzymes and cytoskeleton proteins. In contrast to the large number of metabolic enzymes identified in rat liver within the circled area, few of these were observed in the camel proteome (Fig. 5A). The MS/MS data show the similarity of camel metabolic enzymes to those of other species.

Camel hump fat proteome

The proteome of hump adipose tissue was analyzed in comparison with adipose tissue of rat similar to that of liver (Fig 5B; Tables 4 and 5). Hump fat adipose tissue displayed many more protein spots than that of rat adipose tissue. Unlike the rat control, the proteome of camel adipose tissue contains cytoskeleton proteins together with heat shock proteins, including hsp 27, hsp 70, and vimentin (see insert circled area in Fig. 5B).

These data clearly confirm the presence of actin and tubulin cytoskeletal proteins and high abundance of vimentin, suggesting the overexpression of cytoskeleton proteins in fat cells.

Camel hump adipose tissues also actively perform glycolysis involving the Krebs cycle and hexose monophosphate pathways, as evidenced by the expression of glyceraldehydes-3-phosphate dehydrogenase, isocitrate dehydrogenase, and aldolase. The metabolic enzymes in camel adipose tissue share common domains with other species. The conserved domain of cytochrome b5 in rabbit (gi:164785) shares the same common sequence (40–89 amino acids residues) observed in camel adipose tissue as indicated by MS/MS (Fig. 3B). This finding supports the extensive homology of the conserved domain of this ortholog gene. Moreover, the present investigation suggests the presence of galectin-1 in camel adipose tissue (Fig. 3C). The amino acid residues (residues 69–75) in the reported sequence of galectin-1 in sheep (*Ovis aries*) [gi:3122339] were among those matched by MS/MS to camel.

Camel brain proteome

A number of proteins are uniquely expressed in camel brain with no corresponding protein spots in the equivalent areas of the control. These proteins (Fig. 5C and Table 6) are either uniquely expressed or highly expressed in the brain of camel. The camel brain uniquely expresses or overexpresses chaperonin 10, chaperonin-like beta-synuclein, phosphatidylethanolamine binding protein showing marked homology to bovie brains and cytoskeleton tubulin 5-beta (Fig. 3D).

Camel kidney proteome

Camel kidney revealed only one unique, identifiable spot belonging to calbindin family of proteins (Fig. 5D and Table 7). Many protein spots failed to match the NCBI peptide MS or MS/MS database.

Discussion

The one humped camel has a unique tolerance for extremely hot and arid conditions. The observed climate change with projected environmental increase in global warming and desertation makes the dromedary camel an economically and logistically strategic animal. The absence of genomic data and a defined proteome makes understanding this important species quite challenging. Proteomic data, even in the absence of a defined genome, should lead to improved understanding of the phenotypic acclimatization of this unique mammal. The current study describes a novel approach to understand the interplay between proteome – homeostasis in the dromedary camel.

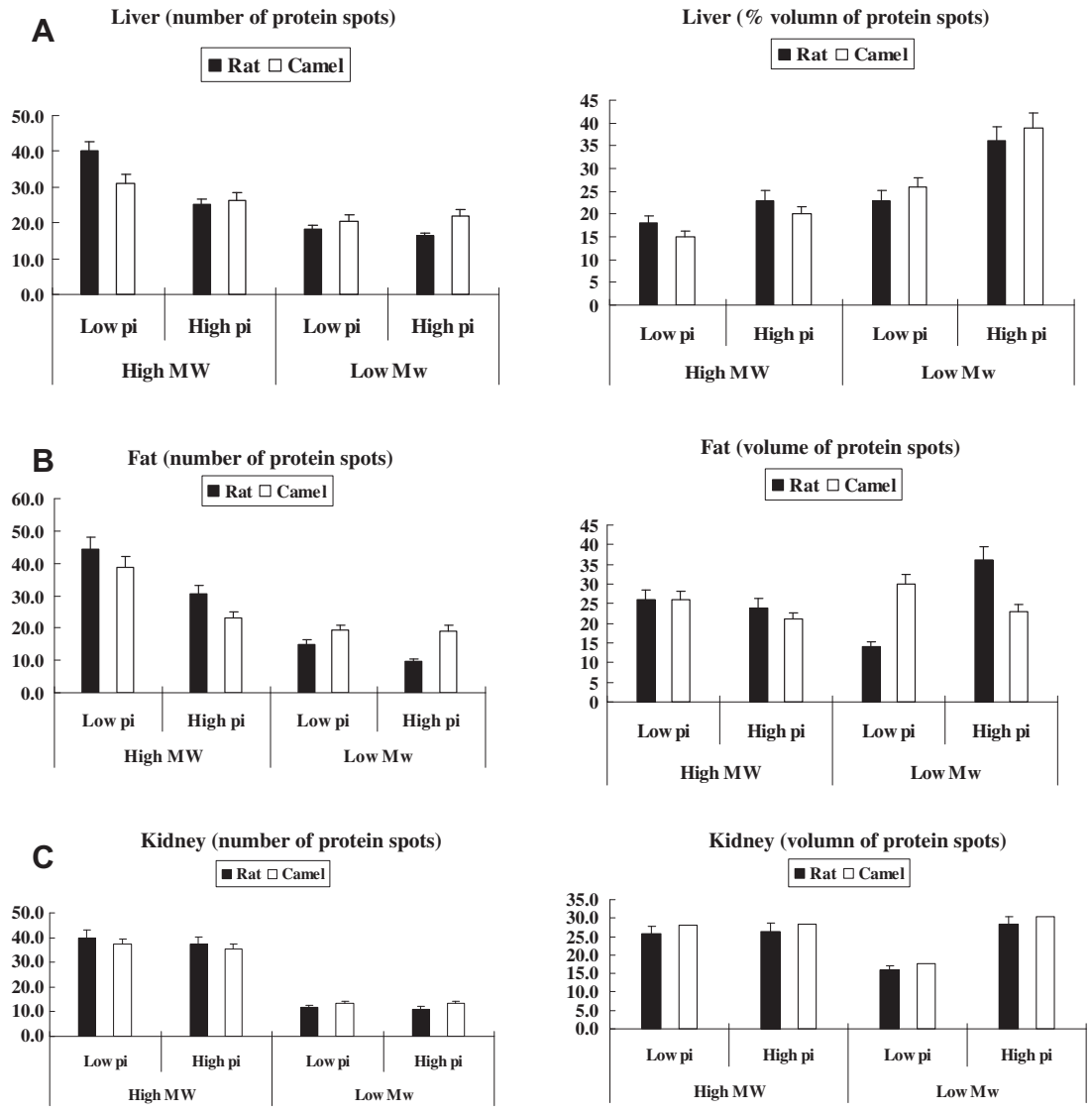

Fig. 4 The relative abundance of proteins (spot numbers and total area) in each quarter of gel that represents the proteomic images. Camel liver (4-A); hump fat (4-B); and kidney (4-C) were estimated from both total number of spots and % volume of occupied proteins (as revealed by the 3D imaging of the gels) in each quarter. The migrated proteins were, therefore, parted according to their MW and pI. The data were then compared with corresponding quarters in rat control. Both adipose tissue and kidney proteomes shared higher clusters of acid tolerable proteins (pI < 7). (Error bars are SEM, $p < 0.05$; $n = 3$ at least).

Camel heart proteome

Energy balance and structural integrity are indispensable elements for the optimal performance of camel heart in an arid environment. Both isocitrate dehydrogenase and ATP synthase considerably impact mitochondrial energizing of the camel heart. The relative increase in isocitrate dehydrogenase parallels a decrease in ATP synthase and represents evidence for proton leakage in camel cardiac muscle. The wide range of body temperature fluctuation accompanied by variable respiratory frequency and different level of exhaled water in desert camel [10] require a greater flexibility of camel mitochondria to move between respiratory states. Further investigation is required on camel mitochondria decoupling proteins to confirm this hypothesis.

Cardiac myocytes contain intracellular cytoskeleton scaffolds that provide for structural support, compartmentalization of intracellular components, protein synthesis, intracellular trafficking, organelle transport within the cell, and second messenger signaling pathway modulation [11,12]. The observed overexpression of cytoskeleton proteins in camel heart greatly reduces cellular stress by offering rapid and durable tool for direct cellular communication [13].

Surprisingly, a marked up-regulation of α-actinin2 expression was observed in camel heart compared to that of the control. Alpha-actinin2 is a cytoskeleton protein belonging to the spectrin gene superfamily. This family has a wide range of cytoskeletal proteins, including the α- and β-spectrins and dystrophins. Alpha-actinin2 is an actin-binding protein with various activities in different cell types. Recent evidence also shows the involvement of α-actinin2 in molecular coupling of a Ca^{2+}-activated K^{+} channel to L-Type Ca^{2+} channels giving better ion channels modulation [14]. This may result in an improved tolerance for abrupt ionic imbalance

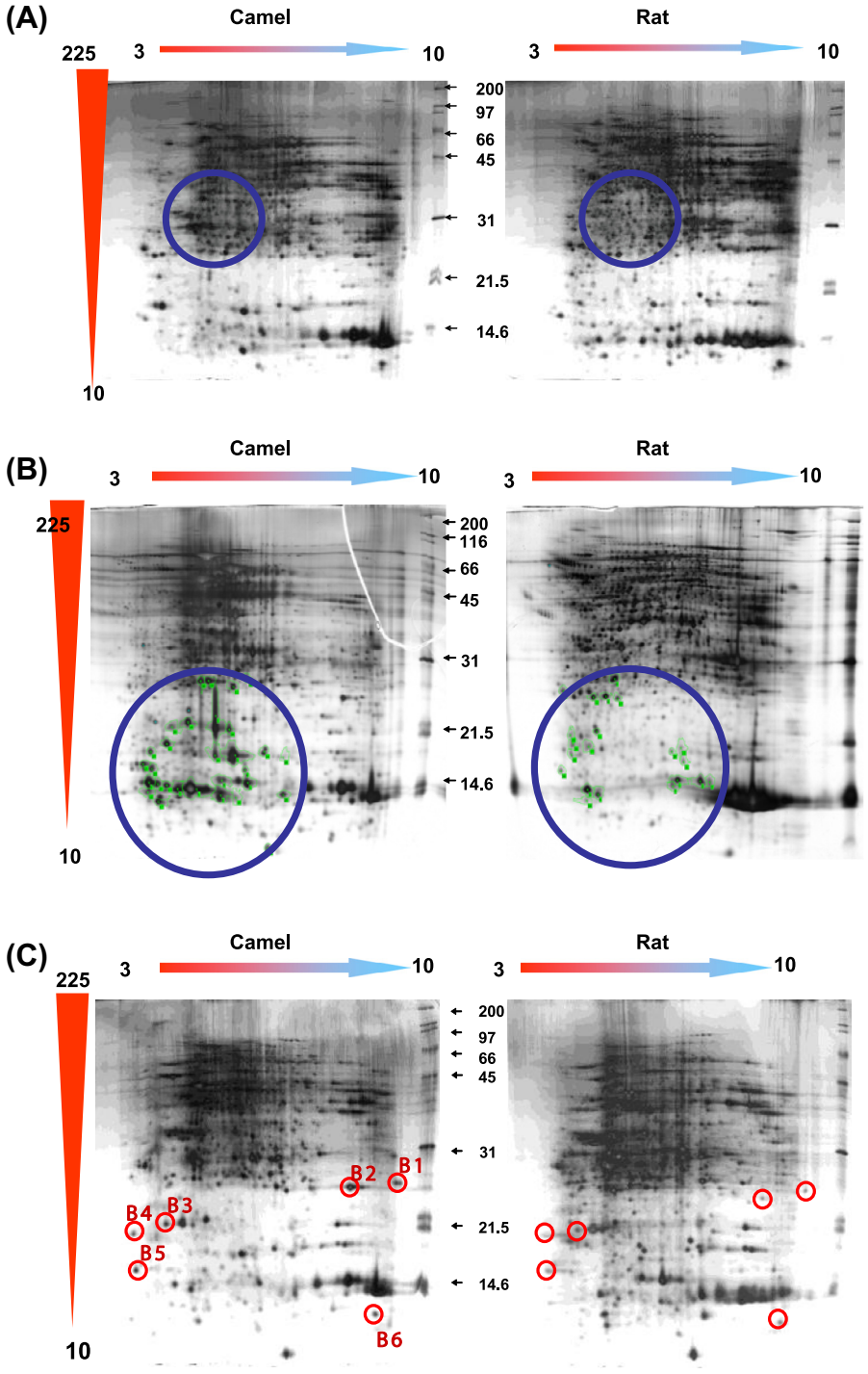

Fig. 5 2D electrophoresis gel images. (A) Camel and rat liver proteomes. Approximately 1314 ± 22 spots were detected within the blue circled area in each gel. The 27 protein spots that showed different expression in camel and rat liver were selected for further MALDI-TOF MS analysis. (B) Adipose tissues of camel hump and rat fat. Approximately 804 ± 32 spots were detected within the blue circle area in each gel. The 26 significantly changed protein spots (marked in green) were selected for further MALDI-TOF MS analysis. (pH range: 3–10; with 10–225 MW range). (C) Brain of camel and rat. Approximately 1476 ± 26.5 spots were detected in each gel. The identified protein spots that showed marked expression in camel brain (red circles) were selected for further MALDI-TOF MS analysis. (D) Kidney of camel and rat, respectively. Approximately 1641.2 ± 12.5 spots were detected in each gel. The identified protein spots that showed marked expression in camel (red circles) over that of control rat (dashed red circles) were selected for further MALDI-TOF MS analysis. (pH range: 3–10; with 10–225 MW range).

with enhanced extra-osmoregulatory capacitance of camel cardiomyocytes.

A sevenfold increase in the expression of alpha B-crystallin fits well with the protection of surrounding structural integrity

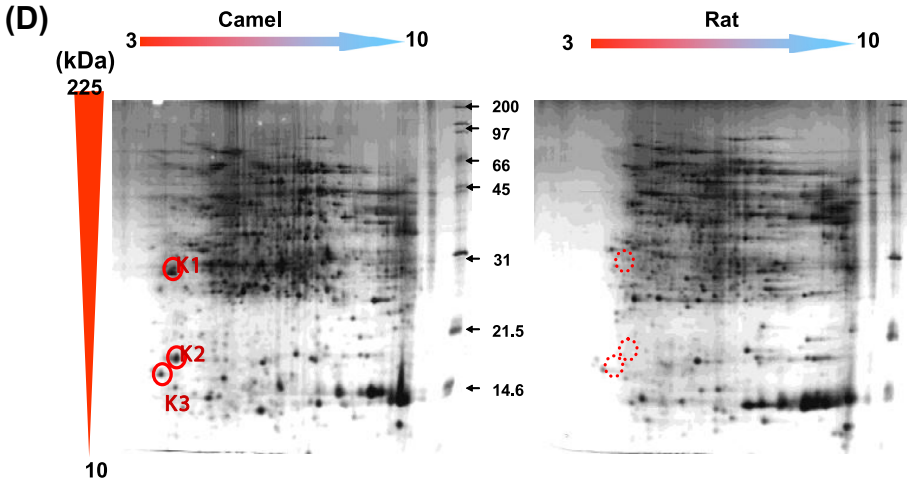

Fig. 5 (*continued*)

Table 2 Identified camel liver proteins in NCBI database search GI; NCBI gene bank ID, Mw; molecular weight, pI; isoelectric point.

Camel liver						
Spot no.	Identified AA sequence (MS/MS)	MATCHED protein	NCBI acc no.	Score	Mr/pI	Seq.cov
C1	R.AVFPSIVGRPR.H K.YPIEHGIVTNWEDMEK.I K.IWHHTFYNELR.V R.VAPEEHPVLLTEAPLNPK.T R.GYSFTTTAER.E K.SYELPDGQVITIGNER.F K.DLYANTVLSGGTTMYPGIADR.M	**Hypothetical protein XP_533132 [*Canis familiaris*] (Actin like protein)**	**73964667**	**114**	**42053/5.24**	27
C2	K.ELFPIAAQVDK.E R.ASSTANLIFEDCR.I K.IAMQTLDMGR.I R.ITEIYEGTSEIQR.L R.LVIAGHLLR.S	**Acyl-CoA dehydrogenase (EC 1.3.99.3) precursor, short-chain-specific**	**111334**	**74**	**44654/8.42**	13
C4	K.LAEQAERYDEMVESMK.K K.KVAGMDVELTVEER.N K.KVAGMDVELTVEER.N R.NLLSVAYK.N R.YLAEFATGNDR.K R.YLAEFATGNDRK.E K.AASDIAMTELPPTHPIR.L K.AASDIAMTELPPTHPIR.L	**PREDICTED: similar to 14-3-3 protein epsilon (14-3-3E) (Mitochondrial import stimulation factor L subunit) (MSF L) isoform 1 [*Canis familiaris*]**	**73960520**	**103**	**26785/4.73**	28
C6,7	K.GAGTDEGCLIEILASR.T R.ISQTYQQQYGR.S R.SLEDDIRSDTSFMFQR.V R.SDTSFMFQR.V R.VLVSLSAGGR.D K.SMKGLGTDDNTLIR.V R.AEIDMLDIR.A R.AEIDMLDIR.A Oxidation (M)	**PREDICTED**:annexin IV isoform 5 [Pan troglodytes]	**114577902**	**79**	**36258/5.84**	23
C8	R.LHDVDFYK.A K.HQLQKDFEQVK.E K.SLDTLQNVSVRLEGLER.D R.ELEAEHQALQR.D R.DLTKQVTVHTR.T R.KAELDELEK.V K.GEYEELHAHTK.E R.SSPTPAEVLTEAK.V	**PREDICTED: similar to DVL-binding protein DAPLE [*Canis familiaris*]**	**73964395**	**71**	266905/5.87	5

(*continued on next page*)

Table 2 (*Continued*)

Camel liver						
Spot no.	Identified AA sequence (MS/MS)	MATCHED protein	NCBI acc no.	Score	Mr/pI	Seq. cov
	K.ASDLPAIGGQPGPPAR.K K.MASSTSEGK.L K.SDEPELLAR.L					
C15,17	M.PGGLLLGDEAPNFEANTTVGR.I R.DFTPVCTTELGR.A K.LAPEFAKR.N K.LPFPIIDDKNR.D K.LSILYPATTGR.N R.NFDEILR.V	**Hypothetical protein [*Macaca fascicularis*]**	84579335	92	25109/5.74	31
	Proteins matching the same set of peptides	Antioxidant protein 2 (non-selenium glutathione peroxidase, acidic calcium-independent phospholipase A2) [*Bos taurus*]	27807167	82	25108/5.74	
C14,16,18	R.SFASSAAFEYIITAK.K R.NSNVGLIQLNRPK.A K.AQFGQPEILIGTIPGAGGTQR.L K.SLAMEMVLTGDR.I K.LFYSTFATEDRK.E K.EGMAAFVEK.R Oxidation (M)	**Enoyl Coenzyme A hydratase, short-chain, 1, mitochondrial [*Bos taurus*]**	**70778822**	80	**31565/ 8.82**	28
	Proteins matching the same set of peptides	Enoyl Coenzyme A hydratase, short-chain, 1, mitochondrial [*Rattus norvegicus*]	17530977	106	31895/6.41	
		Chain A, structure of enoyl-CoA hydratase complexed with the substrate Dac-CoA	20149805	106	28312/6.41	
		Chain A, crystal structure analysis of rat enoyl-CoA hydratase in complex with hexadienoyl-CoA enoyl-CoA hydratase [*Sus scrofa*]	24159081	106	28498/6.41	
C20	R.VLEVGFGMAIAATK.V oxidation (M)	**Guanidinoacetate N-methyltransferase [*Bos taurus*]**	**84370113**	44	**26821/5.70**	5
C27	R.AVAIDLPGLGR.S R.AVAIDLPGLGR.S R.GYVPVAPICTDK.I	**Abhydrolase domain containing 14b [*Rattus norvegicus*]**	**56090461**	72	**22718/5.65**	10

with improved regeneration. The small heat shock protein alpha B-crystallin is a molecular chaperon, which stabilizes proteins that are partially or totally undergo unfolding as a result of inflammatory stress [15]. Alpha B-crystallin, belonging to the family of ATP-independent chaperones, utilizes minimum energy to prevent misfolded target proteins from aggregating and precipitating. Cardiac crystallin is recently proved to contribute in a localized structural or protective role [16]. Furthermore, MAPK kinase MKK6-dependent phosphorylation of alpha B-crystallin shows cytoprotective effects on cardiac myocytes when they are exposed to cellular stress [17]. The overexpression of alpha B-crystallin in camel heart supports this mechanism and suggests an extra protective role against dehydrating and sudden rehydration stress in arid environments. A high level of identity was observed between bovine in both conservative domains of bovine alpha B-crystallin [*Bos taurus*] and the intervening peptides (57–69 aa). These results afford two possible phosphorylation sites in the three major serine residues (Ser19, Ser45, and Ser59) previously shown to be available for post-translational modification [18,19]. Phosphorylation enhances the chaperone activity of alpha B-crystallin, protecting against two types of protein misfolding, amorphous aggregation, and amyloid fibril assembly in the heart [20].

Interestingly, the camel heart proteome shows a relatively similar pattern of distribution of rat heart regarding the localization based on pI scaling and molecular weight distribution.

Proteome interprets the organ uniqueness in liver morphology

Liver is a metabolically active organ contributing in many homeostatic mechanisms. The maintenance of liver activity necessitates the presence of active metabolic and energy saving enzymes, available building blocks, and the safeguarding of the newly formed biomolecules. The hepatic proteome of camel metabolic enzymes indicates a wide range of similarity with other mammals. Energy shuttling enzymes, such as ATP synthase (β-subunit), are similar in the hepatic proteome of camel and other known species. Moreover, energy related and fatty acid regulatory enzymes show a high level of identity to other species. These include citric acid cycle enzymes, NAD-dependent isocitrate dehydrogenase, members of β–oxidation of

Table 3 Identified rat liver proteins in NCBI database search GI; NCBI gene bank ID, Mw; molecular weight, pI; isoelectric point.

Rat liver						
Spot no.	Identified AA sequence (MS/MS)	MATCHED protein	NCBI acc no.	Score	Mr/pI	seq.cov
Metabolic enzymes and enzyme like proteins						
R1,R2	R.RIFSSEHDIFR.E R.IFSSEHDIFR.E K.FFQEEVIPYHEEWEK.A K.CIGAIAMTEPGAGSDLQGVR.T K.AQDTAELFFEDVR.L R.LPASALLGEENKGFYYLMQELPQER.L K.GFYYLMQELPQER.L R.LLIADLAISACEFMFEETR.N	Acetyl-coenzyme A dehydrogenase, long-chain [*Rattus norvegicus*]	6978431	86	48242/7.63	23
R4	K.VADIGLAAWGR.K R.KALDIAENEMPGLMR.M K.ALDIAENEMPGLMR.M R.WSSCNIFSTQDHAAAAIAK.A K.GETDEEYLWCIEQTLHFK.D K.HPQLLSGIR.G K.SKFDNLYGCR.E K.FDNLYGCR.E K.EGNIFVTTTGCVDIILGR.H R.IILLAEGR.L	**Chain A, rat liver S-adenosylhomocystein hydrolase**	**4139571**	**123**	**47889/6.08**	**25**
R6	R.DHGDLAFVDVPNDSPFQIVK.N K.ANEQLAAVVAETQK.N K.DIVYIGLR.D R.DVDPGEHYIIK.T K.VMEETFSYLLGR.K K.VMEETFSYLLGR.K Oxidation (M) R.EGLYITEEIYK.T K.TGLLSGLDIMEVNPTLGKTPEEVTR.T R.EGNHKPETDYLKPPK.-	**Chain A, crystal structure Of the H141c arginase variant complexed with products ornithine and urea**	**13786702**	**125**	**35096/6.72**	**35**
R7,8	R.HIDGAYVYR.N K.LWSTDHDPEMVRPALER.T K.SLGVSNFNR.R K.SLGVSNFNRR.Q K.YKPVTNQVECHPYFTQTK.L R.NPLWVNVSSPPLLKDELLTSLGK.K K.TQAQIVLR.F R.FVEMLMWSDHPEYPFHDEY.-	Aldo-keto reductase family 1, member D1 [*Rattus norvegicus*]	20302063	114	37639/6.18	31

(*continued on next page*)

Table 3 (*Continued*)

Rat liver						
Spot no.	Identified AA sequence (MS/MS)	MATCHED protein	NCBI acc no.	Score	Mr/pI	seq.cov
R9, 11	K.CPGVPSGLETLEETPAPR.L K.THLPLSLLPQSLLDQK.V K.VKVIYIAR.N K.EWWELR.H R.HTHPVLYLFYEDIKENPK.R K.KILEFLGR.S R.SLPEETVDSIVHHTSFK.K R.SLPEETVDSIVHHTSFKK.M K.NTFTVAQNERFDAHYAK.T	**Aryl sulfotransferase [*Rattus norvegicus*]**	**55765**	**134**	**33422/6.41**	**38**
R12	K.IVGSNASQLAHFDPR.V R.VTMWVFEEDIGGR.KOxidation (M) R.KLTEIINTQHENVK.Y K.LTEIINTQHENVK.Y K.FCETTIGCKDPAQGQLLK.E K.ELMQTPNFR.I K.ELMQTPNFR.IOxidation (M) R.ITVVQEVDTVEICGALK.N K.NIVAVGAGFCDGLGFGDNTK.A R.ELHSILQHK.G	**Glycerol-3-phosphate dehydrogenase 1 (soluble) [*Rattus norvegicus*]**	**57527919**	**161**	**38112/6.16**	**32**
R10	R.LGGEVSCLVAGTK.C K.VLVAQHDAYK.G K.QFSYTHICAGASAFGK.N K.LNVAPVSDIIEIK.S R.TIYAGNALCTVK.C K.LLYDLADQLHAAVGASR.A R.AAVDAGFVPNDMQVGQTGK.I K.VVPEMTEILK.K K.VVPEMTEILK.KOxidation (M)	**Electron transferring flavoprotein, alpha polypeptide [*Mus musculus*]**	**31981826**	**114**	**35271/8.42**	**33**
R13,15	K.MKDLHLGEQDLQPETR.E K.MKDLHLGEQDLQPETR.E Oxidation (M) K.AGTTWTQEIVDMIQNDGDVQK.C R.NAKDCLVSYYYFSR.M K.DCLVSYYYFSR.M K.VLWGSWYDHVK.G K.GWWDVKDQHR.I K.FLEKDISEEVLNK.I R.KGMPGDWK.N K.NYFTVAQSEDFDEDYR.R R.KMAGSNITFR.T	**Sulfotransferase family 1A, member 2 [*Rattus norvegicus*]**	**13929030**	**148**	**35855/6.09**	**39**

	R.KMAGSNITFR.TOxidation (M) K.MAGSNITFR.T K.MAGSNITFR.TOxidation (M)					
R14,16	K.DLDVAVLVGSMPR.R K.VIVVGNPANTNCLTASK.S K.SAPSIPKENFSCLTR.L K.NVIIWGNHSSTQYPDVNHAK.V K.EVGVYEALKDDSWLK.G K.GEFITTVQQR.G K.FVEGLPINDFSR.E K.ELTEEKETAFEFLSSA.-	**Malate dehydrogenase, cytoplasmic (cytosolic malate dehydrogenase)**	**92087001**	**116**	**36659/6.16**	**35**
R19	R.LFEENDINLTHIESRPSR.L K.NTVPWFPR.T K.QFADIAYNYR.H R.VEYTEEEKQTWGTVFR.T R.LRPVAGLLSSR.D R.DFLGGLAFR.V R.VFHCTQYIR.H R.TFAATIPRPFSVR.Y	**Chain A, structure of phosphorylated phenylalanine hydroxylase**	**4930076**	**100**	**49694/5.67**	**21**
R20	R.SGVLPWLRPDSK.T K.TQVTVQYVQDNGAVIPVR.V R.VHTIVISVQHNEDITLEAMR.E R.FVIGGPQGDAGVTGR.K K.NFDLRPGVIVR.D K.TACYGHFGR.S	**Methionine adenosyltransferase I, alpha [*Rattus norvegicus*]**	**77157805**	**85**	**44125/5.70**	**21**
R21,22	R.AAVPSGASTGIYEALELR.D K.LAMQEFMILPVGASSFR.E R.IGAEVYHNLK.N K.AGYTDQVVIGMDVAASEFYR.S R.YITPDQLADLYK.S K.VNQIGSVTESLQACK.L R.SGETEDTFIADLVVGLCTGQIK.T R.SFRNPLAK.-	**Enolase 1-like, hypothetical protein LOC433182 [*Mus musculus*]**	**70794816**	**111**	**47453/6.37**	**28**
R23,26	K.NSSVGLIQLNRPK.A K.AFAAGADIKEMQNR.T K.AFAAGADIKEMQNR.T Oxidation (M)	**Chain A, crystal structure analysis of rat enoyl-coA hydratase in complex with hexadienoyl-coA**	**24159081**	**133**	**28498/6.41**	**41**

(*continued on next page*)

Table 3 (*Continued*)

Rat liver						
Spot no.	Identified AA sequence (MS/MS)	MATCHED protein	NCBI acc no.	Score	Mr/pI	seq.cov
	K.FLSHWDHITR.I K.AQFGQPEILLGTIPGAGGTQR.L K.SLAMEMVLTGDR.I K.IFPVETLVEEAIQCAEK.I K.LFYSTFATDDRR.E R.EGMSAFVEKR.K					
R24	-.MAEVGEIIEGCRLPVLR.R Oxidation (M) R.RNQDNEDEWPLAEILSVK.D K.NGLPGSRPGSPEREVPASAQASGK.T R.FNLPKER.E R.MTGSLVSDRSHDDIVTR.M K.TLYYDTDPFLFYVMTEYDCK.G	**PREDICTED: HIV-1 Tat interactive protein, 60 kDa isoform 4 [*Macaca mulatta*]**	**109105458**	**75**	**50824/8.74**	**23**
R27	M.PGGLLLGDEAPNFEANTTIGHIR.F R.FHDFLGDSWGILFSHPR.D R.DFTPVCTTELGR.A K.LAPEFAKR.N K.LIALSIDSVEDHFAWSK.D R.VVFIFGPDKK.L K.LKLSILYPATTGR.N K.LSILYPATTGR.N R.NFDEILR.V R.VVDSLQLTASNPVATPVDWK.K	**Peroxiredoxin 6 [*Rattus norvegicus*]**	**16758348**	**188**	**24860/5.64**	**56**
R29	R.YVQQNAKPGDPQSVLEAIDTYCTQK.E K.EWAMNVGDAK.G K.GQIMDAVIR.E K.GQIMDAVIR.EOxidation (M) R.EYSPSLVLELGAYCGYSAVR.M R.YLPDTLLLEK.C R.KGTVLLADNVIVPGTPDFLAYVR.G K.GTVLLADNVIVPGTPDFLAYVR.G R.GSSSFECTHYSSYLEYMK.V K.AIYQGPSSPDKS.-	**Chain, catechol O-methyltransferase**	**1633081**	**161**	**24960/5.11**	**57**
R28	R.VDYGGVTVDELGK.V	**Phosphatidylethanolamine binding protein [*Rattus norvegicus*]**	**8393910**	**134**	**20902/5.48**	**62**

	K.LYTLVLTDPDAPSR.K K.FREWHHFLVVNMK.G K.FREWHHFLVVNMK.GOxidation (M) K.GNDISSGTVLSEYVGSGPPK.D K.GNDISSGTVLSEYVGSGPPKDTGLHR.Y R.YVWLVYEQEQPLNCDEPILSNK.S K.FKVESFR.K K.YHLGAPVAGTCFQAEWDDSVPK.L					
Other ubiquitous protein						
R3	K.HGDGVKDIAFEVEDCEHIVQK.A K.FAVLQTYGDTTHTLVEK.I R.FWSVDDTQVHTEYSSLR.S R.SIVVANYEESIK.M R.SIVVANYEESIKMPINEPAPGR.K K.MPINEPAPGRK.K K.SQIQEYVDYNGGAGVQHIALR.T R.GMEFLAVPSSYYR.L R.GMEFLAVPSSYYR.L Oxidation (M) R.HNHQGFGAGNFNSLFK.A	**F alloantigen, 4-hydroxyphenylpyruvic acid dioxygenase [*Rattus norvegicus*]**	**202924**	**129**	**43591/6.31**	**34**
R5	R.GRFLHFHSVTFWVGNAK.Q K.HGDGVKDIAFEVEDCEHIVQK.A K.FAVLQTYGDTTHTLVEK.I R.FWSVDDTQVHTEYSSLR.S R.SIVVANYEESIKMPINEPAPGR.K R.GMEFLAVPSSYYR.L R.GMEFLAVPSSYYR.L Oxidation (M) R.HNHQGFGAGNFNSLFK.A	**F alloantigen, 4-hydroxyphenylpyruvic acid dioxygenase [*Rattus norvegicus*]**	**202924**	**82**	**43591/6.31**	**32**
Cytoskeleton						
R18	.PRAVFPSIVGR.S R.AVFPSIVGR.S K.IWHHTFYNELR.V R.VAPEEHPVLLTEAPLNPK.A R.DLTDYLMK.I R.GYSFTTTAER.E K.SYELPDGQVITIGNER.F K.DLYANTVLSGGTTMYPGIADR.M K.IKIIAPPER.K K.IIAPPERK.Y	**Put. beta-actin (aa 27-375) [*Mus musculus*]**	**49868**	**174**	**39446/5.78**	**30**

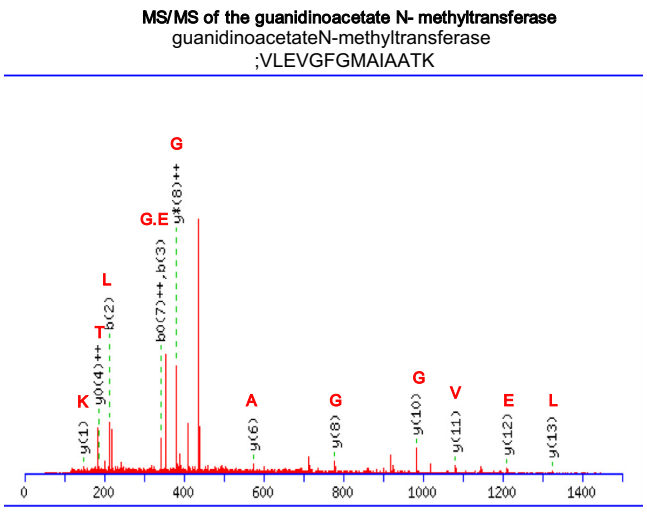

Fig. 6 MS/MS spectrum of the VLEVGFGMAIAATK digested peptide from guanidinoacetate N-methyltransferase. b-ions(b), double charged b-H_2O ion (b^{o++}), y-ions (y), double charged y-NH_3 (y^{*++}), and double charged y-H_2O (y^{o++}) ions of tryptic digestion of peptide VLEVGFGMAIAATK were identified. The ion identification is indicated in spectra panel (Table 8).

fatty acids, including acyl-CoA dehydrogenase and enoyl-CoA hydratase, and even the cholesterol synthesis regulatory enzyme β-hydroxy β-methyl glutaryl CoA reductase.

Camels can tolerate starvation while maintaining a constant nitrogen balance with urea nitrogen recycling [21]. Keeping available nitrogen is essential resource for synthesis of other bioactive nitrogenous molecules including creatine. Creatine phosphate is among the most important energy currency of the cell. This is the first report of enhanced levels of guanidinoacetate methyltransferase in a liver proteome. Guanidinoacetate methyltransferase, a key enzyme of creatine phosphate synthesis, has more protective role on Na^+, K^+-ATPase, and mitochondrial creatine kinase activities and an antioxidant role against lipid peroxidation and guanidinoacetate accumulation [22]. This suggests an additional homeostatic mechanism in camel hepatocytes.

Building new biopolymers is facilitated with guaranteed available energy accompanied by suitable anti-misfolding chaperones and adequate cytoskeleton proteins. Rapid intra- and/or intercellular communication are enforced by the presence of annexin cytoskeleton in camel liver proteome. Antioxidant glutathione peroxidase may afford an extra hepatocellular adaptive mechanism in camel against either heat-induced and/or acid-induced amorphous aggregation of proteins. Mitochondrial import stimulation factor is a known cytoplasmic chaperone specific for mitochondrial precursors [23]. It is related to 14-3-3 protein epsilon. This ubiquitous eukaryotic protein family exhibits a wide range of protein interaction-mediated regulatory and chaperone properties with phosphorylation-dependent affinity. Phosphorylated proteins have much higher affinity when compared with non-phosphorylated ones, explaining the role of 14-3-3 proteins in controlling protein kinases and other cellular events including autophagy and tumorigenesis through Beclin 1 phosphorylation [24,25]. Previous investigation has extended the role of 14-3-3 protein in the interaction with different Na^+/Ca^{2+} exchangers. This maintains a low free Ca^{2+} concentration within the vital cellular limit, by regulating their function, and, as a result, Ca^{2+} signaling in the cell [26].

Hump fat proteome: A dynamic rather than quiescent homeostatic domain

Adipocytes play a central role in energy balance by serving as major site of storage and energy expenditure [27]. The relatively high abundance of low molecular weight and low pI proteins in hump fat suggests an enhanced tolerance toward acidity and a prominent involvement in cellular events. Camel hump fat displayed more proteins than rat adipose tissue, suggesting a more metabolically active tissue. In addition to a well-developed cytoskeleton, containing actin and tubulin, the data confirm the presence and the high levels of vimentin. Moreover, vimentin's essential role in the signal transduction pathway from ss3AR to the activation ERK and its contribution to lipolysis [28] makes vimentin an early marker of adipogenesis. Vimentin regulates lipid droplet content during differentiation [29,30] and controls the key signaling components of lipid raft processing. [31]. Moreover, the higher level of glucagon in camel with consequent elevated basal blood glucose [2] is consistent with the proposed role of vimentin in GLUT-induced adipocyte glucose transport [32]. These data suggest a possible modulating role of adipocyte vimentin for the tolerance of high blood glucose levels in camel. Vimentin might operate as an inducer of a cellular trap for glucose in behalf of adipocyte energy storage. Furthermore, the dynamic nature of vimentin could offer the flexibility of fat cells. Since vimentin provides cells with resilience during mechanical stress *in vivo*, it may response for maintaining cell shape, integrity of its cytoplasm, and stabilizing cytoskeletal interactions. The observed high abundance of vimentin in camel adipocytes could promote the morphology of the hump of the well-nourished camel and can be considered as an adaptive correlate beneficial for living in arid conditions.

Cytochrome b5, a component of dromedary hump tissue, is a membrane bound hemoprotein, which functions as an electron carrier for several membrane bound oxygenases. Its presence in camel fat indicates a well-developed enzymatic system contributing to the detoxification of xenobiotics. Moreover, the conserved domains of cytochrome b5, with rabbit sharing a common sequence (40–89 amino acids residues), supports the extensive homology of this ortholog gene.

Galectin-1, β-galactoside-binding soluble 1 (L-14-I), is a component of dromedary adipocyte. Galectin-1 is widely expressed in epithelial and immune cells, contributing to the control of basic cellular processes, such as proliferation, apoptosis, and signal transduction, and immune modulation [33]. The present investigation suggests a similar role in camel adipocyte metabolism as described for other mammals [34]. The region of interest (residues 69–75) matches carbohydrate-recognition domain. Since the identity of galectin from different mammalian species is 80–90% [35], it is likely that galectin-1 also functions similarly.

Brain proteome

β-Synuclein has been shown to act as chaperonin inhibiting the fibrillation of α-synuclein [36]. The overexpression of β-synuclein in camel brain suggests an additional mechanism to prevent neurodegeneration in brain under intensive environmental stress.

Table 4 Identified camel hump fat proteins in NCBI database search GI; NCBI gene bank ID, Mw; molecular weight, pI; isoelectric point.

Hump fat						
Spot no.	Identified AA sequence (MS/MS)	MATCHED protein	NCBI acc no.	Score	Mr/pI	Seq.cov
Cytoskeleton						
C5	K.SYELPDGQVITIGNER.F K.DLYANTVLSGGTTMYPGIADR.M K.QEYDESGPSVHR.K	Gamma non-muscle actin (*Oryctolagus cuniculus*)	1703	324	41729/5.30	13
	Proteins matching the same set of peptides:	Mostly gamma non-muscle actin and/or actin in many different species	49868 63007 71620	324 324 324	39161 41809 41724	
C11	R.VAPEEHPVLLTEAPLNPK.A R.TTGIVMDSGDGVTHTVPIYEGYALPHAIL	Putative beta-actin (amino acid 27–375) (*Mus musculus*)	49868	123	39161/5.78	13
	Proteins matching the same set of peptides	Actin beta rat Gamma actin (*Mus musculus*)	309090 1335823	123 123	41667 41740	
C30	R.AILVDLEPGTMDSVR.S K.GHYTEGAELVDSVLDVR.K	Unnamed protein product (*Rattus norvegicus*);beta tubulin	57429	84	49931/4.79	7
	Proteins matching the same set of peptides	Beta tubulin (*Homo sapiens*) Beta 3 tubulin (*Gallus gallus*) Predicted similar to tubulin, beta 3 isoform 2 (*Canis familaris*)	158743 1297274 73956775	84 84 84	49812 50485 50648	
Metabolic enzymes and enzyme like protein						
C1	K.EVGVGFATR.K K.NTEISFKLGQEFDEVTDDR.K	Adipocyte lipid-binding protein (*Oryctolagus cuniculus*)	4887137	290	12528/7.71	25
	Proteins matching the same set of peptides	Adipose-type fatty acid binding protein (*Spermophilus tridecemlineatus*) Predicted: simalr to fatty acid binding protein, adipocyte	12802820 73997350	290 290	14756 14687	
C2	MS, 29 peptide Matched from 65	Predicted: similar to centromere protein F	76638067	52	353257/5.01	
C3	MS, 12 peptide matched from 65	mKIAA0421 protein (*Mus musculus*)	37359936	49	76263/7.96	
C4	MS, 11 peptide matched from 65	Predicted: similar to ATP-binding cassette subfamily A member 3, partial [*Danio rerio*].	68424078	61	55936/6.36	
C6	MS, 12 peptide matched from 65	Predicted: similar to type I hair keratin KA27 (*Bos Taurus*)	76649749	47	52545/4.78	
C7	K.NTEISFKLGQEFDEVTDDR.K	Adipocyte lipid-binding protein (*Oryctolagus cuniculus*)	4887137	142	12528/7.71	17
	Proteins matching the same set of peptides	Predicted: similar to fatty acid binding protein, adipocyte	12802820 73997350,	142 142	14756 14687	
C8	MS, 14 peptide matched from 65	Predicted: similar to CG31643-PA isoform 1 (*Bos Taurus*)	76677435	51	96302/8.31	

(*continued on next page*)

Table 4 (*Continued*)

Hump fat						
Spot no.	Identified AA sequence (MS/MS)	MATCHED protein	NCBI acc no.	Score	Mr/pI	Seq.cov
C10	MS, 15 peptide matched from 65	Predicted: similar to protein transport protein Sec2	73952947	44	111485/6.87	
C12	MS, 12 peptide matched from 65	Predicted: similar to aldolase reductase	76662094	52	34311/5.34	
C13	K.DGGAWSGEQR.E K.LPDGYEFK.F	Galectin-1 (beta-galactoside-binding lectin L-14-1) lactose binding lectin 1)	3122339	120	14694/5.37	13
C14	K.LISWYDNEFGYSNR.V	glyceraldehydes-3-phosphate dehydrogenase (*Drosophila hydei*)	11178	118	35359/8.20	4
	Proteins matching the same set of peptides	Glyceraldehydes-3-phosphate dehydrogenase (*Canis familiaris*)	50978862	118	35838	
		Predicted: glyceraldehydes-3-phosphate dehydrogenase (*Pan troglodytes*)	55637711	118	36030	
C16	MS, 10 peptide matched from 65	Apoptosis inhibitor ch-IAPI (*Gallus gallus*)	11991646	46	36543/6.36	
C20	MS, 5 peptide matched from 65	Predicted: similar to mitochondrial ribosomal protein	68437845	51	7433/11.19	
C22	MS, 18 peptide matched from 65	Novel protein similar to vertebrate adenylate cyclase	56207901	54	86625/8.60	
C24	MS, 9 peptide matched from 65	Predicted: similar to ku70-binding protein 3	72014818	50	22290/6.03	
C27	K.FLEEHPGGEEVLR.E R.EQAGGDATENFEDVGHSTDAR.E K.TFIIGELHPDDR.S	Cytochrome b5(sequence coverage 34%, sequence homology in the center of 134 amino acids polypeptide)	117811	156	15340/5.16	34
	Proteins matching the same peptides	Soluble cytochrome b5 (*Oryctolagus cuniculus*)	471150	156	11226	
		Peditoxin, pedin = cytochrome b-like heme protein (*Toxopneustes pileolus*; sea urchin)	837345	156	9453	
C28	MS, 10 peptide matched from 65	Predicted: similar to isocitrate dehydrogenase (NADP)	74005287	49	46777/6.13	
C29	MS, 20 peptide matched from 65	F box and leucine rich repeat protein 10 isoform b	54112380	46	144676/8.74	
Chaperone like proteins						
C15	R.VSLDVNHFAPEELTVK.T	Heat shock protein 27 (*Rattus norvegicus*)	204665	52	22879/6.12	7
	Proteins matching the same peptides	HSP2DT (small heat shock protein (C-terminal) (Mice, peptide partial, 119 aa))	545503	52	12981	
		Heat shock protein 1 (*Mus musculus*)	7305173	52	22887	
C17	R.EMEENFAVEAANYQDTIGR.L R.ISLPLPNFSSLNLR.E	Vimentin (*Homo sapiens*)	37852	106	53653/5.06	7
C18	MS, 10 peptide matched from 65	Heat shock protein hsp70-related protein (*Homo sapiens*)	6563208	49	54744/5.41	
C23	R.EMEENFAVEAANYQDTIGR.L R.EYQDLLNVK.M R.ISLPLPNFSSLNLR.E R.DGQVINETSQHHDDLE	Vimentin	340234	99	35032/4.70	19
	Proteins matching the same peptides	Vimentin (*Pan troglodytes*)	56342340	336	53615	
		Vimentin (*Homo sapiens*)	62414289	336	53619	
C25	R.EMEENFAVEAANYQDTIGR.L R.EYQDLLNVK.M R.ISLPLPNFSSLNLR.E R.DGQVINETSQHHDDLE	Vimentin	340234	86	35032/4.70	19
	Proteins matching the same peptides	Vimentin (*Pan troglodytes*)	56342340	314	53615	
		Vimentin (*Homo sapiens*)	62414289	314	53619	

Other ubiquitous protein						
C19	K.LVNEVTEFAK.G	Albumin precursor (*Felis catus*)	886485	110	68615/5.46	2
	K.YLYEIAR.R					
C9	K.LVNEVTEFAK.G	Albumin precursor (*Felis catus*)	886485	110	68615/5.46	2
	K.LCTVASLR.D					
	Proteins matching the same peptides	Human serum albumin in a complex with myristic acid and tri-iodobenzoic acid	4389275	99	65993	
		Serum albumin (*Homo sapiens*)	28592	99	69321	
C21	K.LVNEVTEFAK.K	Preproalbumin (*Equus cabalus*)	399672	65	68554/5.95	1
	Proteins matching the same peptides	Albumin precursor (*Felis catus*)	886485	95	67837	
		Serum albumin precursor	2492797	64	66429	
C26	K.LVNEVTEFAK.G	Albumin precursor (*Felis catus*)	886485	85	68615/5.46	2
	K.YLYEIAR.R					

Phosphatidylethanolamine binding protein is a lipid-binding protein that enhances acetylcholine synthesis with additional inhibitory action on MEK- and ERK-signaling pathways. Phosphatidylethanolamine binding protein in camel brain shows high homology to the bovine protein. Furthermore, the larger amounts found in camel brain when compared to rat brain do not show the same proteome spot, suggesting enhanced ERK signaling in camel brain, warranting further study.

Camel proteome and heat shock proteins

Despite a preliminary investigation on a 73 kDa heat shock protein (hsp 73) in camel [37], there are no recent reports on hsp in camel. In the current study, proteins with extensive homology to the hsp 65, hsp 27, and chaperonin 10 were found in various camel organs. Heat shock proteins defense against dehydration or thermal stress in arid environments.

General outlook and implication of a well-developed cytoskeleton

The entire economy of the cell is a function of the structure of its transport facilities. Cytoskeletal proteins sculpt the structural architecture of cells and are classified into three groups: microfilaments represented in our data finding by actin filaments; intermediate filaments e.g. vimentin as that found in hump fat cells; and microtubules as different kind of β-tubulin. Different cytoskeletal protein monomers can build into a variety of structures based on associated proteins. Actin filaments are dynamic with their length controlled by polymerization driven through nucleotide hydrolysis. Additionally, actin filaments act with microtubules as railroads for motor proteins carrying transport vehicles, unfolded/misfolded proteins, and chromosomes important for cell-cell communication and survival [13]. Widely distributed adherence junctions are self-assembled cadherins interacting with ß-catenin, which binds α-catenin and in turn interact with the actin cytoskeleton [38]. Their overexpression in the heart together with actin enhances intracellular communication. In non-muscle cells, the cytoskeletal isoform is found along with microfilament bundles and adherence junctions that bind actin to the membrane. The almost tenfold increase in α-actinin2 expression in camel heart and the presence of β-tubulin as a major energy determent cytoskeleton in the camel brain confers stress adaptation to the camel while guaranteeing more flexibility in ion channel modulation [13] to keep pace with abrupt ionic imbalances associated with dehydration–rehydration cycles.

Cytoskeleton-cellular signaling possible interplay

The DVL-binding protein DAPLE and the marked expression of actins suggest a possible interplay between cytoskeleton and fine tuning of intracellular signaling in camel hepatic cells. DAPLE binds to Dvl and functions as a negative regulator of the Wnt signaling pathway [39]. The Wnt pathway (known as the wingless pathway in *Drosophila*) has a role in organ development in a number of species [40] with the potential of carcinogenesis development on sudden activation [41]. The inductive properties of Wnt signaling are mediated by setting free actin-bound β-catenin. The accumulated β-catenin is then translocates to the nucleus where it binds to T-cell factors and activates transcription of a

Table 5 Identified protein spots of adipose tissue of rat in NCBI database search GI; NCBI gene bank ID, Mw; molecular weight, pI; isoelectric point.

Rat fat						
Spot no.	Identified AA sequence (MS/MS)	MATCHED protein	NCBI acc no.	Score	Mr/pI	Seq. cov
Cytoskeleleton						
R2	K.SYELPDGQVITIGNER.F K.DLYANTVLSGGTTMYPGIADR.M K.DLYANTVLSGGTTMYPGIADR.M K.QEYDESGPSIVHR.K K.QEYDESGPSIVHR.K	Putative beta-actin (aa 27–375) (*Mus musculus*)	49868	308	39161/5.78	14
Metabolic enzymes and enzyme like proteins						
R3	K.DSNNLCLHFNPR.F K.DDGYWGTEQR.E R.ETAFPFQPGSITEVCITFDQADLTIK.L R.LNMEAINYMAADGDFK.I	Beta-galactoside-binding lectin (*Rattus norvegicus*)	9845261	124	14847/5.14	47
	Proteins matching the same peptides	Beta-galactoside-binding lectin (*Rattus norvegicus*)	9845261	333	14847	
R4	R.WVTYFNKPDIDAWELR.K R.LNDFASAVR.I	Cytochrome c oxidase	6680986	129	16020/6.08	17
	Proteins matching the same peptides	Cytochrome c oxidase, subunit Va (*Rattus norvegicus*)	24233541	129	16119	
R5	K.MVVECVMNNAICTR.V	C-fatty acid binding protein (*Rattus norvegicus*)	546420	61	15050/6.14	10
R6	R.KEGGLGPLNIPLLADVTK.S K.EGGLGPLNIPLLADVTK.S R.QITVNDLPVGR.S	Peroxiredoxin 2 (*Rattus norvegicus*)	34849738	74	21784/5.34	14
	Proteins matching the same peptides	Peroxiredoxin 2 (*Rattus norvegicus*)	360324	208	21778	
R7	K.LVSSENFDDYMK.E K.LGVEFDEITPDDR.K K.LGVEFDEITPDDRK.V	Adipocyte fatty acid binding protein (*Rattus norvegicus*)	1658525	133	14699/7.71	19
R8	K.FDASFFGVHPK.Q R.LLLEVSYEAIVDGGINPASLR.G R.GTNTGVWVGVSGSEASEALSR.D R.DPETLLGYSMVSCQR.A	Fatty acid synthase (*Rattus norvegicus*)	57890	313	272478/5.96	2
R9	K.ITQFCHHFLEGK.I K.NFEEVAFDEK.K	Prolyl 4-hydroxylase, beta polypeptide (*Rattus norvegicus*)	38197382	75	56916/4.82	4
	Proteins matching the same peptides	Prolyl 4-hydroxylase, beta polypeptide (*Rattus norvegicus*)	56916	75	56916	

R12	R.KEGGLGPLNIPLLADVTK.S R.QITVNDLPVGR.S R.QITVNDLPVGR.S	Type II peroxiredoxin 1 (*Mus musculus*)	3603241	55	21778/5.20	14
	Proteins matching the same peptides	Perodiredoxin 2 (*Rattus norvegicus*)	8394432	55	21770	
		Peroxiredoxin 2 (*Mus musculus*)	31560539	55	21834	
R14	K.LFDHPEVPIPAESESV	Fatty acid synthase (*Rattus norvegicus*)	57890	68	272478/5.96	1
R20	K.GDGPVQGVIHFEQK.A R.VISLSGEHSIIGR.T	Cu/Zn superoxide dismutase (EC 1.15.1.1)	207012	174	15700/5.88	17
	Proteins matching the same peptides	Cu/Zn superoxide dismutase(*Rattus norvegicus*)	1213217	174	16006	
		Cu/Zn superoxide dismutase (*Rattus norvegicus*)	8394328	174	15902	
R21	R.VTMWVFEEDIGGR.K R.VTMWVFEEDIGGR.K	Glycerophosphate dehydrogenase	387178	47	37560/6.75	3
	Proteins matching the same peptides	Glycerol-3-phosphate dehydrogenase (NAD+), cytoplasmic	3023880	47	37373	
		Glycerol-3-phosphate dehydrogenase 1 (soluble) (*Rattus norvegicus*)	57527919	47	37428	
Cellular signaling related marcromolecules						
R10	K.TVEEAENIVVTTGVVR	Gamma synuclein (*Mus musculus*)	58651748	99	13152/4.68	13
R11	K.DVFLGTFLYEYSR.R R.RHPDYSVSLLLR.L K.LGEYGFQNAILVR.Y K.APQVSTPTLVEAAR.N	Alpha fetoprotein	191765	303	47195/5.47	12
Other ubiquitous protein						
R15	R.LPCVEDYLSAILNR.L R.RPCFSALTVDETYVPK.E K.AADKDNCFATEGPNLVAR.S	Albumin (*Rattus norvegicus*)	19705431	116	68674/6.09	7

Table 6 Identified proteins camel brain in NCBI database search GI; NCBI gene bank ID, Mw; molecular weight, pI; isoelectric point.

Brain						
Spot no.	Identified AA sequence (MS/MS)	Matched protein	NCBI acc no.	Score	Mr/pI	Seq.cov
B1	K.FSPLTSNLINLLAENGR.L	H + -ATPase subunit, OSCP = oligomysin sensitivity conferring protein	913531	51	20932/9.76	8
	Proteins matching the same peptides	H + -ATPase subunit, OSCP = oligomysin sensitivity conferring protein [swine, heart, peptide mitochondrial	913531	51	20932	
		Mitochondrial ATP synthase, O subunit [*Bos taurus*]	27806307	51	23449	
		Similar to oligomycin-sensitivity conferral protein [*Bos taurus*]	28189911	51	14199	
		ATP synthase, H + transporting, mitochondrial F1 complex, O subunit (oligomycin-sensitivity conferring protein) [*Bos taurus*]	74268299	51	23419	
B2	K.LYTLVLTDPDAPSR.K K.GNNISSGTVLSDYVGSGPPK.G	Phosphatidylethanolamine binding protein 1 (PEBP-1) (HCNPpp) (Basic cytosolic 21 kDa protein) [contains: Hippocampal cholinergic neurostimulating peptide (HCNP)]	1352725	148	21087/6.9	18
	Proteins matching the same peptides	Chain, phosphatidylethanolamine binding protein from calf brain	4389366	148	20828	
		Chain A, structure of the phosphatidylethanolamine binding protein from bovine brain	6729706	148	20956	
		Phosphatidylethanolamine binding protein [*Bos taurus*]	75812940	148	21106	
B3	R.IMNTFSVVPSPK.V + Oxidation (M) R.AVLVDLEPGTMDSVR.S R.AVLVDLEPGTMDSVR.S + Oxidation (M) R.AVLVDLEPGTMDSVR.S + Oxidation (M) R.INVYYNEATGGNYVPR.A R.INVYYNEATGGNYVPR.A	Tubulin 5-beta [*Homo sapiens*]	35959	193	50055/4.81	9
	Proteins matching the same peptides	Tubulin, beta-4 [*Homo sapiens*]	21361322	193	50010	
		Tubulin, beta-4, isoform CRA_b [*Homo sapiens*]	119589485	193	54946	
B4	K.EGVVQGVASVAEK.T K.EGVVQGVASVAEK.T	Beta-synuclein (phosphoneuroprotein 14) (PNP 14) (14 kDa brain-specific protein)	464424	67	14268/4.4	9
	Proteins matching the same peptides	Beta-synuclein (phosphoneuroprotein 14) (PNP 14)	2501106	67	14495	
		Beta-synuclein [*Homo sapiens*]	4507111	67	14279	
B5	K.AQSELLGAADEATR.A	Chain H, bovine F1-ATPase inhibited by Dccd (dicyclohexylcarbodiimide)	11514063	55	15056/4.53	9
	Proteins matching the same peptides	ATP synthase, H + transporting, mitochondrial F1 complex, delta subunit precursor [*Bos taurus*]	28603800	55	17601	
B6	K.VLLPEYGGTK.V K.VLQATVVAVGSGSK.G	Chaperonin 10 [*Homo sapiens*]	4008131	127	10576/9.44	24

Table 7 Identified proteins camel kidney in NCBI database search GI; NCBI gene bank ID, Mw; molecular weight, pI; isoelectric point.

Kidney						
Spot no.	Identified AA sequence (MS/MS)	MATCHED protein	NCBI acc no.	Score	Mr/pI	Seq. cov
K1	R.TDLALILSAGDN.-K.LAEYTDLMLK.L + Oxidation (M) R.LLPVQENFLLK.F	Calbindin	575508	145	18613/4.6	20
	Proteins matching the same peptides	Unnamed protein product [*Mus musculus*]	26347175	145	30247	
		Calbindin-d28 k	203237	143	30225	
		Calbindin-28 K [*Mus musculus*]	6753242	143	30203	
		Cerebellar Ca-binding protein, spot 35 protein [*Rattus norvegicus*]	14010887	143	30203	

Table 8 The ion identification as indicated in spectra panel.

Ion type	Neutral Mr
a	[N] + [M] – CHO
a*	a-NH_3
a°	a-H_2O
b	[N] + [M] – H
b*	b-NH_3
b°	b-H_2O
c	[N] + [M] + NH_2
d	a – Partial side chain
v	y – Complete side chain
w	z – Partial side chain
x	[C] + [M] + CO – H
y	[C] + [M] + H
y*	y-NH_3
y°	y-H_2O
z	[C] + [M] – NH_2

number of genes. Overexpressed actin is in accord with the favored homeostasis.

Conclusions

The present investigation tried to shed light on camel proteome as innovative central point to study mammalian evolution. Much of the data obtained for camel cannot fit with proteomics data for other mammals. This mismatch is not an artifact but rather support the peculiarity of the camel and in particular its adaptive nature. This study also confirms the conserved nature of many camel proteins. Thus, the camel proteome corresponds to a remote reference useful in developing a perspective of proteomic evolution among different species.

Conflict of interest

The authors have declared no conflict of interest.

Acknowledgement

The authors are grateful for Dr. Moustafa Radwan for helpful assistance of this work.

Appendix A. Supplementary material

Supplementary data associated with this article can be found, in the online version, at http://dx.doi.org/10.1016/j.jare.2013.03.004.

References

[1] Ali AY. The Meaning of the Holy Qur'an; Amana Publications. ASIN: B004H0G2P6, 2004; Sura 88, verse17.
[2] Abdel-Fattah M, Amer H, Ghoneim MA, Warda M, Megahed Y. Response of one-humped camel (*Camelus dromedarius*) to intravenous glucagon injection and to infusion of glucose and volatile fatty acids, and the kinetics of glucagon disappearance from the blood. Zentralbl Veterinarmed 1999;A(46):473–81.
[3] Eitan A, Aloni B, Livne A. Unique properties of the camel erythrocyte membrane, II. Organization of membrane proteins. Biochem Biophys Acta 1976;426:647–58.
[4] Warda M, Zeisig R. Phospholipid- and fatty acid-composition in the erythrocyte membrane of the one-humped camel [*Camelus dromedarius*] and its influence on vesicle properties prepared from these lipids. Dtsch Tierarztl Wochenschr 2000;107:368–73.
[5] Davidson A, Jaine T, Vannithone S. The Oxford companion to food. 2nd ed. USA: Oxford University Press; 15 October 2006. p. 68, 129, 266, 762. ISBN:0192806815.
[6] Hamers-Casterman C, Atarhouch T, Muyldermans S, Robinson G, Hamers C, Songa EB, et al. Naturally occurring antibodies devoid of light chains. Nature 1993;363:6428–46.
[7] Kim N, Lee Y, Kim H, Joo H, Youm JB, Park WS, et al. Potential biomarkers for ischemic heart damage identified in mitochondrial proteins by comparative proteomics. Proteomics 2006;6:1237–49.
[8] Gay S, Binz PA, Hochstrasser DF, Appel RD. Modeling peptide mass fingerprinting data using the atomic composition of peptides. Electrophoresis 1999;25:3527–34.
[9] Zubarev R, Mann M. On the proper use of mass accuracy in proteomics. Mol Cell Proteomics 2007;6:377–81.
[10] Schmidt-Nielsen K, Crawford EC, Hammel HT. Respiratory water loss in camel. Proc R Soc Lond (B Biol Sci) 1981;211:291–303.
[11] Ryan SD, Ferrier A, Kothary RA. Novel role for the cytoskeletal linker protein dystonin in the maintenance of microtubule stability and the regulation of ER-Golgi transport. Bioarchitecture 2012;1:2–5.
[12] Calaghan SC, Le Guennec JY, White E. Cytoskeletal modulation of electrical and mechanical activity in cardiac myocytes. Prog Biophys Mol Biol 2004:29–59.

[13] Usui T. Actin- and microtubule-targeting bioprobes: their binding sites and inhibitory mechanisms bioscience. Biotechno Biochem 2007;71(2):300–8.
[14] Lu L, Timofeyev V, Li N, Rafizadeh S, Singapuri A, Harris TR, Chiamvimonvat N. Alpha-actinin2 cytoskeletal protein is required for the functional membrane localization of a Ca^{2+}-activated K^+ channel (SK2 channel). Proc Natl Acad Sci 2009;106(43):18402–7.
[15] Narayan P, Meehan S, Carver JA, Wilson MR, Dobson CM, Klenerman D. Amyloid-β oligomers are sequestered by both intracellular and extracellular chaperones. Biochemistry 2012;20(46): 9270–6.
[16] Bousette N, Chugh S, Fong V, Isserlin R, Kim KH, Volchuk A, et al. Constitutively active calcineurin induces cardiac endoplasmic reticulum stress and protects against apoptosis that is mediated by alpha-crystallin-B. Proc Natl Acad Sci 2010;107:18481–6.
[17] Hoover HE, Thuerauf DJ, Martindale JJ, Glembotski CC. Alpha B-crystallin gene induction and phosphorylation by MKK6-activated p38. A potential role for alpha B-crystallin as a target of the p38 branch of the cardiac stress response. J Biol Chem 2000;275:23825–33.
[18] Smith JB, Sun Y, Smith DL, Green B. Identification of the posttranslational modifications of bovine lens alpha B-crystallins by mass spectrometry. Protein Sci 1992;1:601–8.
[19] Voorter CE, de Haard-Hoekman WA, Roersma ES, Meyer HE, Bloemendal H, De Jong WW. The *in vivo* phosphorylation sites of bovine alpha B-crystallin. FEBS Lett 1989;259:50–2.
[20] Ecroyd H, Meehan S, Horwitz J, Aquilina JA, Benesch JL, Robinson CV, et al. Mimicking phosphorylation of alpha B-crystallin affects its chaperone activity. Biochem J 2007;401:129–41.
[21] Mousa HM, Ali KE, Hume ID. Comp Biochem Physiol A 1983;74:715–20.
[22] Kolling J, Wyse AT. Creatine prevents the inhibition of energy metabolism and lipid.
[23] Komiya T, Hachiya N, Sakaguchi M, Omura T, Mihara K. Recognition of mitochondria-targeting signals by a cytosolic import stimulation factor, MSF. J Biol Chem 1994;269:30893–7.
[24] Wang RC, Wei Y, An Z, Zou Z, Xiao G, Bhagat G, et al. Akt-mediated regulation of autophagy and tumorigenesis through Beclin 1 phosphorylation. Science 2012;6(6109):956–9.
[25] Mackintosh C. Dynamic interactions between 14-3-3 proteins and phosphoproteins regulate diverse cellular processes. Biochem J 2004;381:329–42.
[26] Pulina MV, Rizzuto R, Brini M, Carafoli E. Inhibitory interaction of the plasma membrane Na^+/Ca^{2+} exchangers with the 14-3-3 proteins. J Biol Chem 2006;281:19645–54.
[27] Spiegelman BM, Flier JS. Obesity and the regulation of energy balance. Cell 2001;104:531–43.
[28] Kumar N, Robidoux J, Daniel KW, Guzman G, Floering LM, Collins S. Requirement of vimentin filament assembly for beta 3-adrenergic receptor activation of ERK MAP kinase and lipolysis. J Biol Chem 2007;282:9244–50.
[29] Brasaemle DL, Dolios G, Shapiro L, Wang R. Proteomic analysis of proteins associated with lipid droplets of basal and lipolytically stimulated 3T3-L1 adipocytes. J Biol Chem 2004;45:46835–42.
[30] Al Battah F, De Kock J, Ramboer E, Heymans A, Vanhaecke T, Rogiers V, Snykers S. Evaluation of the multipotent character of human adipose tissue-derived stem cells isolated by Ficoll gradient centrifugation and red blood cell lysis treatment. Toxicol *In Vitro* 2011;25:1224–30.
[31] Meckes Jr DG, Menaker NF, Raab-Traub N. Epstein-Barr virus LMP1 modulates lipid raft microdomains and the vimentin cytoskeleton for signal transduction and transformation. J Virol 2013;87:1301–11.
[32] Guilherme A, Emoto M, Buxton JM, Bose S, Sabini R, Theurkauf WE, et al. Perinuclear localization and insulin responsiveness of GLUT4 requires cytoskeletal integrity in 3T3-L1 adipocytes. J Biol Chem 2000;275:38151–9.
[33] Dettin L, Rubinstein N, Aoki A, Rabinovich GA, Maldonado CA. Regulated expression and ultrastructural localization of galectin-1, a proapoptotic beta-galactoside-binding lectin, during spermatogenesis in rat testis. Biol Reprod 2003;68:51–9.
[34] Kiwaki K, Novak CM, Hsu DK, Liu FT, Levine JA. Galectin-3 stimulates preadipocyte proliferation and is up-regulated in growing adipose tissue. Obesity 2007;15:32–9.
[35] Barondes SH, Cooper DN, Gitt MA, Galectins Leffler H. Structure and function of a large family of animal lectins. J Biol Chem 1994;269:20807–10.
[36] Yamin G, Munishkina LA, Karymov MA, Lyubchenko YL, Uversky VN, Fink AL. Forcing nonamyloidogenic beta-synuclein to fibrillate. Biochemistry 2005;44:9096–107.
[37] Ulmasov HA, Karaev KK, Lyashko VN, Evgen'ev MB. Heat-shock response in camel (*Camelus dromedarius*) blood cells and adaptation to hyperthermia. Comp Biochem Physiol B 1993;106:867–72.
[38] Nelson WJ, Nusse R. Convergence of Wnt, beta-catenin, and cadherin pathways. Science 2004;303:1483–7.
[39] Oshita A, Kishida S, Kobayashi H, Michiue T, Asahara T, Asashima M, et al. Identification and characterization of a novel Dvl-binding protein that suppresses Wnt signalling pathway. Genes Cells 2003;8:1005–17.
[40] Shackel N. Zebrafish and the understanding of liver development: the emerging role of the Wnt pathway in liver biology. Hepatology 2007;45:540–1.
[41] Giles RH, van Es JH, Clevers H. Caught up in a Wnt storm: Wnt signaling in cancer. Biochem Biophys Acta Rev Cancer 2003;1653:1–24.